0 0 0 0 4 8 0 0 4 3 3

Submitted to Nuclear Physics A

RECEIVED
LAWRENCE
LABORATORY

MAR 8 1978

LIBRARY AND
DOCUMENTS SECTION

UC-34C
LBL-6534 Rev.
Preprint c.1

OBSERVATIONS IN THE REACTION OF TWO MAGIC NUCLEI: ^{208}Pb AND ^{48}Ca

J. M. Nitschke, R. E. Leber, M. J. Nurmia, and
A. Ghiorso

January 1978

Prepared for the U. S. Department of Energy
under Contract W-7405-ENG-48

For Reference

Not to be taken from this room

LBL-6534 Rev.
c.1

DISCLAIMER

This document was prepared as an account of work sponsored by the United States Government. While this document is believed to contain correct information, neither the United States Government nor any agency thereof, nor the Regents of the University of California, nor any of their employees, makes any warranty, express or implied, or assumes any legal responsibility for the accuracy, completeness, or usefulness of any information, apparatus, product, or process disclosed, or represents that its use would not infringe privately owned rights. Reference herein to any specific commercial product, process, or service by its trade name, trademark, manufacturer, or otherwise, does not necessarily constitute or imply its endorsement, recommendation, or favoring by the United States Government or any agency thereof, or the Regents of the University of California. The views and opinions of authors expressed herein do not necessarily state or reflect those of the United States Government or any agency thereof or the Regents of the University of California.

0 0 0 0 4 8 0 3 4 3 6

LBL-6534
(revised)

OBSERVATIONS IN THE REACTION OF TWO MAGIC NUCLEI: ^{208}Pb AND ^{48}Ca*

J. M. Nitschke, R. E. Leber, M. J. Nurmia, and A. Ghiorso

Lawrence Berkeley Laboratory, University of California
Berkeley, California 94720

ABSTRACT

Excitation functions for compound-nucleus and transfer reactions have been measured with ^{48}Ca ions on ^{208}Pb targets. A comparison is made with the ^{40}Ar-on-^{208}Pb reaction to explain the observed anomalous behavior of the transfer reactions and a surprising cutoff of the (^{48}Ca, 3n) exit channel. The former effect is interpreted as an enhancement of the tunneling gap between the projectile and the target while the latter is seen as a consequence of the angular momentum of the compound nucleus.

INTRODUCTION

All attempts to detect superheavy nuclides synthesized in nuclear reactions have failed thus far in spite of efforts to come as close as possible to the predicted island of stability by using the neutron-rich projectile ^{48}Ca to bombard the neutron-rich target ^{248}Cm.[1] The possible reasons for this lack of success fall into two categories:

a. The half-lives of the nuclides produced may be so short that present experimental techniques have failed to detect them. This could be due to the shell stabilization at Z = 114 and N = 184 being weaker than predicted; it could also be due to the fact that even the ^{48}Ca + ^{248}Cm scheme will only produce neutron-deficient isotopes off the island of

stability and their fission barriers may be so narrow that even small shape distortions will lead to instantaneous fission.

b. The actual formation cross sections of the expected nuclei may have been below the experimental limits of detection. Apart from a rather hopeless "fission catastrophe" caused by insufficient strength of the shell effects per se, this could well be due to the high angular momenta and high excitation energies of the compound nuclei which would reduce their fission barriers to dangerously low values.

Present experimental results are not sufficient to exclude any of the above possibilities or their combinations. We have therefore performed experiments designed to study one of the critical points — the influence of the excitation energy and the angular momentum on the survival of the compound nucleus. During this work we have also observed an unexpected behavior of multiple-nucleon transfer reactions.

Magic nuclei deserve special consideration for use as targets and projectiles since they facilitate the formation of compound nuclei with the least possible amount of excitation energy[2]). Due to the filling of major particle shells the shell effect[3]) in ^{208}Pb is - 10 MeV and that in ^{48}Ca is -1.9 MeV. This leads in their combination to a compound nucleus with a minimum excitation energy of 26.1 MeV. We have studied the reaction between these nuclei and compared it with the reaction of ^{208}Pb with ^{40}Ar; the latter has a shell effect of +2.5 MeV and the minimum excitation energy of the compound nucleus is 36.4 MeV.

EXPERIMENTAL

The experimental technique, described in detail elsewhere[4]) makes use of transporting nuclei in a stream of helium seeded with sodium chloride aerosol particles. The activity passes through a teflon capillary to be deposited on a vertical magnesium wheel which is stepped at a predetermined rate, positioning the activity spots in front of seven surface barrier detectors. The information obtained from the detectors is processed by a computer. The targets consisted of 1 mg/cm^2 ^{208}PbO deposited on 4.5 mg/cm^2 palladium-covered molybdenum foils. PbO was preferred over Pb metal or PbS due to its better thermal stability. The maximum target temperature was limited through the use of a gas cooling system[5]) and monitored by an infrared sensor. Typical beam current densities were 6μA(electrical)/cm^2. The details of accelerating ^{48}Ca ions are described elsewhere.[6])

RESULTS

Excitation functions for the ^{208}Pb(HI,xn) reactions and for transfer products in the Bi-Po region were measured with both ^{40}Ar and ^{48}Ca projectiles and are shown in fig. 1. The same figure shows calculated cross sections obtained with the JORPL code.[7]) This code calculates neutron-evaporation cross sections without explicitly considering de-excitation by γ decay, a fact which is crucial to understanding its failure to correctly predict the result of the ^{48}Ca on ^{208}Pb experiment. The evaporation-residue results are also summarized in Table I.

The following observations are pertinent to the results of the Ar on Pb experiment shown in fig. 1a.

1. The 3n evaporation product ^{245}Fm is identified by its half-life of 4.5 ± 0.6 ($T_{1/2}^{lit}$ = 4.2 sec) and its alpha energy E_α = 8.15 ± 0.02 MeV (E_α^{lit} = 8.15 MeV) as shown in fig. 2. Its peak cross section of 15 ± 5nb at 198 MeV agrees well with the calculated value of 18.6 nb at 197.5 MeV.

2. The alpha particles of the 2n evaporation product, ^{246}Fm are not observed above a detection limit of 2nb. This result is at variance with the observation of a 1 sec spontaneous-fission activity by Oganessian et al[8]) which was produced with a peak cross section of 7 nb and attributed to the ∿10% SF branching of ^{246}Fm.

3. A 3ms SF activity was observed in a later experiment[9]) and is possibly due to the (Ar,4n) reaction product, ^{244}Fm. All observed cross sections are in agreement with JORPL calculations.

While the ^{40}Ar on ^{208}Pb reaction shows the expected behavior, the ^{48}Ca bombardment (fig. 1b) displays two striking effects:

1. The transfer reaction products ^{211}Bi, ^{211m}Po, and ^{212m}Po are observed at <u>higher</u> energies than the compound nucleus evaporation residue ^{254}No and reach the microbarn level significantly <u>above</u> the reaction barrier contrary to ^{40}Ar on ^{208}Pb and many other reactions investigated in the past.

2. The 3n evaporation product ^{253}No for which the JORPL code predicts a cross section of 6μb is not observed above a detection limit of 20nb. The 2n evaporation residue ^{254}No identified by its α-energy and half-life (fig. 3) is seen with a peak cross section of 3.4 ± 0.4 μb

at 227 MeV bombarding energy in agreement with findings of Flerov et al.[10]) but again in poor agreement with JORPL calculations of 0.45 μb at 223 MeV. Further, the 2n excitation curve is wider than expected from calculations.

DISCUSSION OF THE TRANSFER REACTIONS

In the $^{48}Ca + ^{208}Pb$ experiment in which the anomalous behavior of the transfer reactions was observed, we intended to study compound nucleus products. We therefore have no information about the kinematic parameters of the transfer reactions and can only attempt to investigate the coarsest feature of the experimental results which is the displacement of the onset of the multinucleon transfer reactions with respect to the complete fusion barrier. In the following it is not our aim to describe the absolute behavior but rather the relative differences between the ^{40}Ar and ^{48}Ca reactions.

A characteristic of the heavy ion reactions under question is that the wavelength of the relative motion of the projectile is short compared to the sum of the nuclear radii ($\lambda_{Ca} \approx 0.06$ fm compared to $R_{Ca} + R_{Pb} \approx 12$ fm) which is equivalent to the statement that the Sommerfeld parameter η is large compared to unity. This localization leads to the concept of well-defined classical trajectories; further, the cross section for transfer in a collision of two nuclei moving on classical scattering orbits will be proportional to the product of the probability for scattering and the probability for the cluster to tunnel from one nuclear potential to the other.[11])

$$\sigma(\theta) = |f_{tr}(\theta)|^2 = |f_{sc}(\theta)|^2 \cdot |f_{tun}(\theta)|^2 \qquad (1)$$

The second factor is proportional to the probability of finding the cluster outside of the nucleus and can be calculated from the overlap of the initial and final states. For a reaction of the form $A+a \rightarrow B+b$: $f_{tun}(\theta) = \langle\psi_B\psi_b|V|\psi_A\psi_a\rangle$. Expressing the state function ψ as a product a radial and an angular term

$$\psi = f(r)\ Y_{LM}(\vartheta,\phi)$$

one obtains the radial wave equation

$$\frac{1}{r^2}\frac{d}{dr}\left(r^2\frac{df}{dr}\right) + \left[\kappa^2 - \frac{L(L+1)}{r^2}\right] f = 0 \quad . \tag{2}$$

For the "interior" region of a square well potential with depth V_o, κ^2 is defined as:

$$\kappa^2 = \frac{2\mu}{\hbar^2}(V_o - E_B).$$

μ is the reduced mass and E_B the binding energy of the transferred particle. Of interest here is the "exterior" case where $V(r) = 0$ and

$$\kappa^2 = \frac{2\mu}{\hbar^2} E_B \tag{3}$$

The solution of eq. 2 for this case can then be expressed in terms of spherical Hankel functions of the first kind $h_L^{(1)}(i\kappa r)$:

$$\psi(r) \propto \exp\left[\frac{i\pi}{2}(L+2)\right] h_L^{(1)}(i\kappa r) \quad .$$

Hankel functions for $L > 0$ contain sums of terms of the form $(\kappa r)^{-n}$ and since in our case κ is in the order of 1 fm^{-1} and r is the order of 10 fm we can neglect these terms and obtain an asymptotic solution which is valid for all L values and depends only on the binding energy:

$$\psi \propto \frac{\exp(-\kappa r)}{\kappa r} \tag{4}$$

Combining this expression with the classical equation for scattering and assuming that the transfer occurs at the minimum distance R_{min} eq. (1) becomes an approximate expression for the transfer reaction cross section:

$$\frac{d\sigma}{d\theta} \cong S^B \, S^b \, N_B \, N_b \, \frac{C}{q^4} \, e^{-2\kappa R_{min}} \tag{5}$$

Here S and N are spectroscopic and normalization factors respectivel, for a reaction of the type A + a → B + b, q is the transferred momentum: $q \cong (2/\lambda\!\!\!^{-})\sin\theta/2$. From eq. 4 an exponential rise of the transfer cross section with decreasing minimum distance is expected up to a radius R_a where strong interactions set in, leading to complete fusion and inelastic processes. For many experimental cases the interaction radius R_a can be calculated from $R_a = r_o\,(A_1^{1/3} + A_2^{1/3})$ with values for r_o between 1.6 and 1.7 fm. The constant part of the transfer excitation function is of no concern for the present discussion, but rather the displacement with respect to the interaction radius, an effect which is contained in the exponential term of eq. 5. For convenience we introduce the following transformation:

$$R_{min} = R_o(\text{target}) + R_o(\text{projectile}) + S$$

where R_o corresponds to the point of half-maximum density of individual nuclei: $R_o = r_o\,A^{1/3}$ with $r_o = 1.07$ [12]. The term $e^{-\kappa S}$ then is proportional to the probability of finding a particle or a particle cluster

at a distance S outside the nuclear surface defined by R_o. If we now require that the probability of finding a cluster at the surface of the target nucleus (^{208}Pb) be independent of whether the cluster originates from a ^{48}Ca or ^{40}Ar nucleus, schematically $(e^{-\kappa S})_{Ca} = (e^{-\kappa S})_{Ar}$ we obtain the following condition for the tunneling gap

$$S_{Ca} = S_{Ar} \cdot \kappa_{Ar}/\kappa_{Ca} \quad , \tag{6}$$

κ_{Ar} and κ_{Ca} are related to the binding energy in the projectile via eq. 3. The distances between the nuclear surfaces are calculated from

$$S^* = R_B(L) - R_o(\text{target}) - R_o(\text{projectile}). \tag{7}$$

$R_B(L)$ corresponds to point where the interaction potential between the two nuclei reaches a maximum ($dV(r)/dr = 0$); it is also the point of highest transfer probability. The interaction potential $V(r)$ is calculated as a sum of the conventional Coulomb and centrifugal terms plus a proximity force term[13] representing the strong interaction (fig. 4). A question of fundamental concern is whether the cluster in a multinuclear transfer reaction is "preformed inside the projectile" and transferred to the target nucleus as a sub-unit or whether the individual wavefunctions of the nucleons overlap at the surface of the target nucleus. The experimental results presented here allow us to answer this question.

Under the preformation hypothesis we calculate as an example the displacement of the α-transfer reactions as follows: the binding energy of a ^4He cluster as calculated from experimental mass values[14] is 14.38 MeV in ^{48}Ca and 6.80 MeV in ^{40}Ar. Applying eq. 3 yields

$\kappa_{Ca}^{4He} = 1.589$ and $\kappa_{Ar}^{4He} = 1.083\ fm^{-1}$ and from eq. 7 we obtain $S_{Ar}^{*} = 1.95$ fm. Equation 6 then gives $S_{Ca} = 1.33$ fm. This value has to be compared with S_{Ca}^{*} calculated from eq. 7 as 2.02 fm, which implies that for an S-wave interaction the ^{48}Ca nucleus is $\Delta S_{Ca} = S_{Ca}^{*} - S_{Ca} = 2.02 - 1.33 = 0.69$ fm too far away from the Pb nucleus to yield a transfer probability for the ^{4}He cluster equal to the $^{40}Ar + {}^{208}Pb$ case. In order to augment the transfer probability the ^{48}Ca has to move closer to the Pb nucleus without "going over the top of the barrier", which requires that the increase in nuclear force be balanced by a larger centrifugal force. <u>This can only be achieved with an increase in bombarding energy</u>. From fig. 4b and fig. 5 we calculate that the energy to displace the top of the barrier is $\partial V_B/\partial r = -65.2$ MeV/fm.*) Moving the ^{48}Ca and the ^{208}Pb nucleus closer together by $\Delta S_{Ca} = 0.69$ fm requires therefore an additional energy of $0.69 \cdot 65.2 = 45$ MeV(!). This would correspond to observing transfer reactions in the $^{40}Ar + {}^{208}Pb$ case at about 122 MeV in clear contradiction to the experimental results. The above assumption of a "preformation" of the ^{4}He cluster can therefore not be correct.

In the following we will work with the hypothesis that the wave-functions of individual nucleons overlap at the surface of the target nucleus. The exponential term in eq. 5 then has to be replaced by the product of the exponentially decaying wavefunctions of the n "individual" nucleons:

---

*$\partial V_B/\partial r$ is not very sensitive to the specific choice of the interaction potential: Using a potential published by R. Bass[15] we obtain $\partial V_B/\partial r = -60.0$ MeV/fm.

$$e^{-2\kappa R_{min}} \Rightarrow e^{-2\kappa_1 R_{min}} \cdot e^{-2\kappa_2 R_{min}} \cdot \ldots e^{-2\kappa_n R_{min}}$$

$$= e^{-2\bar{\kappa} R_{min}}$$

where $\bar{\kappa} = \kappa_1 + \kappa_2 + \ldots \kappa_n$

and eq. 6 becomes:

$$S_{Ca} = S_{Ar} \cdot \bar{\kappa}_{Ar}/\bar{\kappa}_{Ca} \qquad (8)$$

In calculating κ for an individual nucleon it is assumed that its binding energy is not affected by the fact that other nucleons are "preparing" for transfer. We are taking the transfer of a ^{4}He cluster again as an example: The neutron and proton binding energies in ^{48}Ca are 9.95 and 15.81 MeV respectively, this yields $\kappa^n_{Ca} = 0.683$ fm^{-1} and $\kappa^p_{Ca} = 0.861$ fm^{-1}. For ^{4}He we then have $\bar{\kappa}_{Ca}^{2n2p} = 2 \cdot 0.683 + 2 \cdot 0.861 = 3.088$ fm^{-1} and in a similar calculation for ^{40}Ar $\bar{\kappa}_{Ar}^{2n2p} = 2.890$ fm^{-1}. Applying eq. 8: $S_{Ca} = 1.95 \cdot 2.89/3.09 = 1.83$ fm. Now $\Delta S_{Ca} = S^*_{Ca} - S_{Ca} = 2.02 - 1.83 = 0.19$ fm and $\Delta S_{Ca} \cdot |\partial V_B/\partial r| = 0.19 \cdot 65.2 =$ 12.4 MeV, which is substantially different from the previously calculated value of 45 MeV. The associated increase in rotational energy corresponds to an incremental orbital momentum of about 58 $\hbar$. In order to get a visual impression of the viability of the above treatment we have subtracted 12.4 MeV from the data points for the ^{208}Pb(^{48}Ca,^{40}Ar)^{212m}Po

reaction in Fig. 1b, multiplied the result by the ratio of the interaction barriers 162.5/179.9 = 0.903 and plotted these calculated points in fig. 1a. Similar calculations were performed for the two other transfer reactions leading to ^{211}Bi and ^{211m}Po and the results also plotted in fig. 1a. The agreement with the data points of the ^{40}Ar on ^{208}Pb reaction is now within the resolution of the experiment. Closer inspection of fig. 1a also reveals that the "reversal" of the Bi-Po cross sections between the two reactions is correctly reproduced.

It can be argued that the formation of the transfer products in the ^{48}Ca reaction can proceed via a different path compared to the ^{40}Ar case. We have therefore calculated the Q-values for the reactions leading to ^{211}Bi, ^{211m}Po, and ^{212m}Po, as well as the optimum Q-values.

Q_{opt} was obtained by setting $R_o = R^i_{min} = R^f_{min}$ and $p_i\ (k_i,\eta_i,L_i,R_o) \cong p_f\ (k_f,\eta_f,L_f,R_o)$ which leads to the condition:[16]

$$Q_{opt} = -(E^i_{CM} - E^f_{CM})$$

$$= -E^i_{CM}\left(1-\frac{\mu_i}{\mu_f}\right)-\left[V_i^C(R_o)\,\frac{\mu_i}{\mu_f} - V_f^C(R_o)\right]$$

$$-\left[V_i^N(R_o)\,\frac{\mu_i}{\mu_f} - V_f^N(R_o)\right] - \hbar^2\left[\frac{L_i(L_i+1) - L_f(L_f+1)}{2\mu_f\,R_o^2}\right] \qquad (4)$$

where indices i and f refer to the initial and the final state, p is the radial momentum, μ are reduced masses, and superscripts C and N refer to the Coulomb and the nuclear potential. The nuclear potential is of the Woods-Saxon type:

$$V^N(r) = \frac{V_o}{1+\exp((r-R)/a)}$$

with $R = r_o(A_1^{1/3} + A_2^{1/3})$, $V_o = -40$ MeV, $V_o = 1.31$ fm and $a = 0.45$.

$Q_{opt}(\ell)$ for the three transfer reactions is plotted in fig. 6 and the reaction Q-values indicated by arrows. The following observations can be made:

(1) For low ℓ-values the reactions are strongly mismatched.

(2) ^{48}Ca requires higher angular momenta for matching then ^{40}Ar. This fact is distinct from the similar requirement for a higher angular momentum to obtain a narrower tunneling gap as discussed earlier.

(3) The Q-values for the ^{48}Ca reactions are 4 to 7 MeV lower than for ^{40}Ar, but as can be seen from fig. 6 this is mostly due to rotational energy, and will not necessarily lead to the evaporation of an additional neutron.

This becomes even more evident from fig. 7 where the optimum Q-values are compared to the yrast line (in this example for ^{211}Bi) using the rigid rotor value for the moment of inertia. The cross-hatched area above the yrast line is the γ-cascade band calculated for a neutron binding energy of 4.4 MeV,[17] and Q_{opt}-values are taken from fig. 6a. As can be seen Q_{opt} lies for $\ell = 0$ only 0.5 MeV above

and for higher ℓ-values within the γ-cascade band. Neutron evaporation is therefore unlikely unless the transfer process proceeds in a highly unmatched fashion. No reason can be seen that the unmatched process should be preferred for Ar and not for Ca or vice versa. Another argument against the evaporation of a neutron can be derived if one contrary to the previous discussion still maintains the idea of a preformed cluster transfer. In the case of ^{211}Bi and ^{212m}Po ^{4}H and ^{5}He would have to be transferred; both particles are however unbound.

DISCUSSION OF THE COMPLETE FUSION RESULTS

Over the past years we have built up considerable confidence in our CN-cross-section code JORPL, and several mechanisms were considered to explain the large discrepancy between the calculated and observed 3n cross section in the ^{48}Ca on ^{208}Pb reaction, among them: precompound evaporation effects, enhanced tunneling, possible shell effects in the reaction mechanism, superfluidity, pairing effects and others. The most satisfying interpretation however is based on angular momentum considerations, and can best be visualized in the grazing-collision (GC) picture. For a detailed description see Klapdor et al.[18]). In fig. 8 we have applied this model to the ^{40}Ar + ^{208}Pb $\rightarrow$ ^{245}Fm reaction, showing the maximum orbital angular momentum (J_{max}) which can be brought in by the ^{40}Ar projectile for an excitation energy of 39 MeV ($E_p^{c.m.}$= 168 MeV) and the maximum angular momentum which can be removed by the 3n-pseudo-particle. As demonstrated in many examples in Refs. 18-21, and substantiated by Hauser-Feshbach calculations, a large fraction of the cross sections of a reaction lies within the inverted "half parabola" (fig. 8). The vertex of the

half parabola defined by L_{in}^{graz} and L_{out}^{graz} is given by $E = E_p^{cm} + Q - V_c$, with E_p^{cm} the projectile energy in the center of mass system, Q the Q-value, and V_c the Coulomb barrier in the exit channel. For the evaporation of neutrons E is equal to the excitation energy of the compound nucleus.

We now consider the de-excitation process of the compound nucleus which can in principle proceed via the emission of neutrons, charged particles, γ-rays, or all three. The minimum levels which the nucleus can occupy at a given angular momentum are bounded by the yrast line E(J). The yrast line for ^{245}Fm was scaled from measured values for ^{238}U,[22] assuming an $A^{5/3}$ dependence; which yields $E(J) = 5.84\ J^2$ (KeV)*. The region important for γ-decay ("γ-cascade band") is located between the yrast line and a line drawn approximately one neutron binding energy above and labeled $k_\gamma = 0.5$. Within a few tenths of MeV below the $k_\gamma = 0.5$ line γ-decay takes over almost completely and becomes the main de-excitation process.[23] The cross section ratio $\sigma/\sigma_{max} = \sigma_{CF}(J)/\sigma_{CF}(J_{max})$ is shown in fig. 8 as a horizontal bar at $E^* = 39$ MeV and if each neutron removes on the average about 10 MeV the principal reaction channel open at this energy is 3nγ with 4nγ being possible at higher energies. The 2nγ reaction channel leading to ^{246}Fm has to be considerably suppressed since the minimum excitation energy for ^{40}Ar on ^{208}Pb is 36 MeV.

---

*This expression might not be correct at higher J values where the moment of inertia approaches the rigid rotor value.[25]

The GC picture for ^{48}Ca on ^{208}Pb is shown in fig. 9. Before comparing it to the ^{40}Ar on ^{208}Pb case we have to consider that the angular momentum brought in by the projectile cannot be larger than the critical angular momentum. This is the case for the GC-curve associated with E = 30 MeV (E_p^{cm} = 184 MeV) fig. 9, where the critical angular momentum as calculated from[24]

$$J_{crit} = \left(\frac{\sigma_{CF}^{(mb)} A_p A_T \cdot E^{cm}}{651.23(A_p+A_T)}\right)^{1/2} \qquad (5)$$

is 30ħ[†] while L_{Ca}^{graz} is 53ħ. For the case of E = 40 MeV (E_p^{cm} = 194 MeV) the maximum angular momentum is determined by the grazing limit (L_{Ca}^{graz} = 82ħ). The yrast line for ^{254}No is again extrapolated from uranium: $E(J) = 5.43\ J^2(keV)^*$. The principal reaction channel is now 2nγ and only a very small fraction of the total cross section due to low ℓ-waves could possibly result in the evaporation of 3 neutrons. This effect is not very sensitive to the excitation energy which might account for the unusually large width of the excitation function. Charged-particle emission is completely prohibited: the GC curves for protons and alpha particles (labeled L_p^{graz} and L_α^{graz}) are below the yrast line. (Our experimental limits are $\sigma(^{48}Ca,p) \leqq 360$ nb and $\sigma(^{48}Ca,\alpha) \leq 30$ nb.) The (^{48}Ca,1n) reaction is suppressed because the minimum excitation energy is 26 MeV. (Our experimental limit is 35 nb.) After the evaporation of two neutrons almost all de-excitation channels terminate within the γ-cascade band. The JORPL code which does not explicitly take γ-deexcitation and yrast levels into account will fail when -- as in the ^{48}Ca case -- a large fraction of the excitation

---

[†]The complete-fusion cross section σ_{CF} in eq. 5 was obtained from the JORPL calculations adjusted to reproduce the experimentally determined 2n cross section.

energy is in the form of rotational energy. Applications of the code in the past involved excitations of 40 to 50 MeV and/or low angular momenta brought in by light projectiles so that the evaporation of neutrons was not restricted. Under these conditions the code predicted -- as in the ^{40}Ar-on-^{208}Pb case -- the cross section successfully.

The ratio of the peak cross sections $\sigma(^{48}\mathrm{Ca},2n)/\sigma(^{40}\mathrm{Ar},3n)$ is $(3.4 \cdot 10^{-30})/(15 \cdot 10^{-33}) \cong 230$, and is mainly due to fission competition, witnessed by the fact that the ratio

$$\frac{\Gamma_n/\Gamma_f(^{256}\mathrm{No}^*) \cdot \Gamma_n/\Gamma_f(^{255}\mathrm{No}^*)}{\Gamma_n/\Gamma_f(^{248}\mathrm{Fm}^*) \cdot \Gamma_n/\Gamma_f(^{247}\mathrm{Fm}^*) \cdot \Gamma_n/\Gamma_f(^{246}\mathrm{Fm}^*)} = 150$$

as calculated with a formula proposed by Sikkeland et al.[20]). If this figure is multiplied by the ratio of the complete fusion cross sections the peak cross section ratio becomes 205, in agreement with the experiment.

CONCLUSION

The observed shift of the onset of the transfer reactions with respect to the complete fusion barrier in the case of ^{48}Ca on ^{208}Pb has been interpreted as an enhanced tunneling gap. The narrowing of this gap is associated with an increase in orbital angular momentum and a higher bombarding energy. The "cut-off" of the 3nγ-reaction channel in the same reaction can be understood by considering the limits imposed by the available excitation energy and the yrast levels of the compound nucleus.

The authors are thankful to Drs. N. K. Glendenning and F. S. Stephens for inspiring discussions.

REFERENCES

*This work was done with support from the U.S. Department of Energy.

1. E. K. Hulet, R. W. Lougheed, J. F. Wild, J. H. Landrum, P. C. Stevenson, A. Ghiorso, J. M. Nitschke, R.J. Otto, D.J. Morrissey, P. A. Baisden, B. F. Gavin, D. Lee, R. J. Silva, M. M. Fowler, G. T. Seaborg, Phys. Rev. Lett. 39, 385 (1977).
2. Yu. Ts. Oganessian, Yu. P. Tretyakova, A. S. Iljinov, A. G. Demin, A. A. Pleve, S. P. Tretykova, V. M. Plotko, M. P. Ivanov, N. A. Dalinov, Yu. S. Korotkin, G. N. Flerov, Dubna Preprint D7-8099 (1974).
3. W. D. Myers and W. J. Swiatecki, UCRL-11980 (1965).
4. A. Ghiorso, J. M. Nitschke, J. R. Alonso, C. T. Alonso, M. Nurmia, G. T. Seaborg, E. K. Hulet, R. W. Lougheed, Phys. Rev. Lett. 33, 1490 (1974).
5. J. M. Nitschke, Nucl. Inst. Meth. 138, 393 (1976).
6. B. F. Gavin, IEEE Transactions on Nucl. Science NS-23, 1008 (1976).
7. J. R. Alonso, Gmelin: Handbuch der Anorganischen Chemie, 7b, 28 (1974).
8. Yu. Ts. Oganessian, Y. P. Tretyakova, A. S. Iljinov, A. G. Demin, A. A. Pleve, S. P. Tretykova, V. M. Plotko, M. P. Ivanov, N. A. Danilov, Yu. S. Korotkin, N. G. Glerov, JINR D7-8099 (1974).
9. K. E. Williams, private communication.
10. G. N. Flerov, Yu. Ts. Oganessian, A. A. Pleve, N. V. Pronin, Yu. P. Tretyakov, JINR D7-9555 (1976).
11. W. von Oertzen, Nucl. Spectroscopy and Reactions, (ed. J. Cerny), Part B, p. 292 (1974).

12. R. Hofstadter, Ann. Rev. Nucl. Sci., 7, 231 (1957).

13. J. Błøcki, J. Randrup, W. J. Swiatecki, C. F. Tsang, LBL-5014, to be published in Ann. of Physics 1977.

14. Atomic Data and Nucl. Data Tables 17, 411 (1976).

15. R. Bass, Phys. Lett. 47B, 139 (1973).

16. W. von Oetzen, Nucl. Spectroscopy and Reactions, (ed. J. Cerny), Part B, p. 315 (1974).

17. W. D. Myers and W. J. Swiatecki, UCRL-11980 (1965).

18. H. V. Klapdor, G. Rosner, H. Reiss, M. Schrader, Nucl. Phys. A244, 157 (1975).

19. H. V. Klapdor, H. Reiss, G. Rosner, M. Schrader, Phys. Lett. 49B, 431 (1974).

20. H. V. Klapdor, H. Willmes, Phys. Lett. 62B, 395 (1976).

21. H. V. Klapdor, H. Reiss, G. Rosner, Nucl. Phys. A262, 157 (1976).

22. E. Gross, J. deBoer, R. M. Diamond, F. S. Stephens, P. Tjøm, Phys. Rev. Lett. 35, 565 (1975).

23. J. R. Grover, J. Gilat, Phys. Rev. 157, 814 (1967).

24. S. Cohen, F. Plasil, W. J. Swiatecki, Ann. of Phys. 82, 557 (1974).

25. F. S. Stephens, private communication.

26. T. Sikkeland, A. Ghiorso, M. Nurmia, Phys. Rev. [2] 172, 1232 (1968).

TABLE I

Reaction	$\sigma_{calc}(E_p^{lab})$	$\sigma_{exp}(E_p^{lab})$	in nb(MeV)
$^{208}Pb\ (^{40}Ar,2n)^{246}Fm$	0.1(197)	< 2	
$,3n)^{245}Fm$	19(198)	15±5(198)	(peak)
$,4n)^{244}Fm$	3(207)	2.5(207)	(single point)
$^{208}Pb\ (^{48}Ca,1n)^{255}No$	1(223)	$\leq$ 35	
$,2n)^{254}No$	450(223)	3400±400(227)	(peak)
$,3n)^{253}No$	6000(226)	$\leq$ 20	
$,p\ )^{255}Md$	-	$\leq$ 360	
$,\alpha\ )^{252}Fm$	-	$\leq$ 30	

FIGURE CAPTIONS

Fig. 1 Measured and calculated (dashed lines) excitation functions for the reaction $^{208}Pb(^{40}Ar,xn)^{248-x}Fm$ (a) and $^{208}Pb(^{48}Ca,xn)^{256-x}No$ (b) and associated transfer reactions. The curves drawn through the solid symbols (Fig. 1a) are calculated from ^{48}Ca on ^{208}Pb results (see text).

Fig. 2 Decay curve of ^{245}Fm formed in the reaction $^{208}Pb(^{40}Ar,3n)$.

Fig. 3 Decay curves for ^{254}No formed in the reaction $^{208}Pb(^{48}Ca,2n)$.

Fig. 4 Interaction potential V(r) for ^{40}Ar on ^{208}Pb (a) and ^{48}Ca on ^{208}Pb for different values of angular momentum (b).

Fig. 5 V(r) for ^{48}Ca on ^{208}Pb on a larger scale to determine $\partial V(r)/\partial r$.

Fig. 6 Optimum Q-values (Q_{opt}) as a function of orbital angular momentum (ℓ) for the three transfer reaction products.

Fig. 7 The optimum Q-values (Q_{opt}) for the reaction $^{208}Pb\ (^{48}Ca,^{45}K)^{211}Bi$ and $^{208}Pb(^{40}Ar,^{37}C\ell)^{211}Bi$ in relation to the yrast line for ^{211}Bi.

Fig. 8 Grazing collision picture for the reaction $^{208}Pb\ (^{40}Ar,3n)^{245}Fm$ at an excitation energy of 39 MeV. The yrast line is calculated from $E(J) = 5.84\cdot10^{-3}J^2$ MeV. The horizontal bar at $E^* = 39$ MeV indicates the fraction of the total fusion cross section as a function of J in a sharp cut-off model. The γ-cascade band is drawn for a neutron binding energy of 8 MeV.

Fig. 9 Grazing collision picture for the reaction $^{208}Pb\ (^{48}Ca,2n)^{254}No$ for two different excitation energies (30 MeV and 40 MeV) with yrast line E(J), cascade band limit $k_\gamma = 0.5$, and rigid rotor calculation of the yrast line $E(J)_{rr}$.

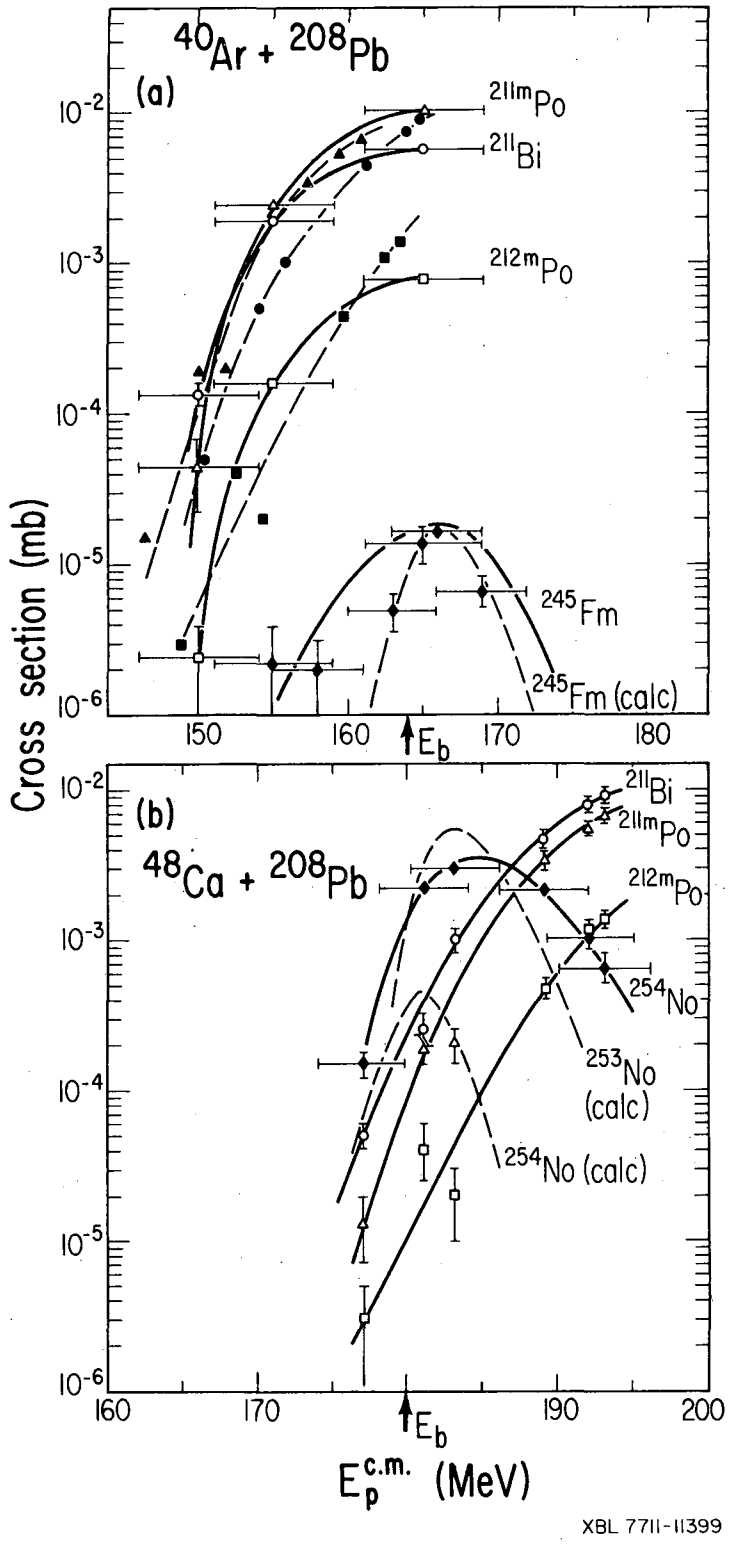
40Ar + 208Pb
(a)
211mPo
211Bi
212mPo
245Fm
245Fm (calc)
Eb
(b)
48Ca + 208Pb
211Bi
211mPo
212mPo
254No
253No (calc)
254No (calc)
Cross section (mb)
Ep c.m. (MeV)
XBL 7711-11399

Fig. 1

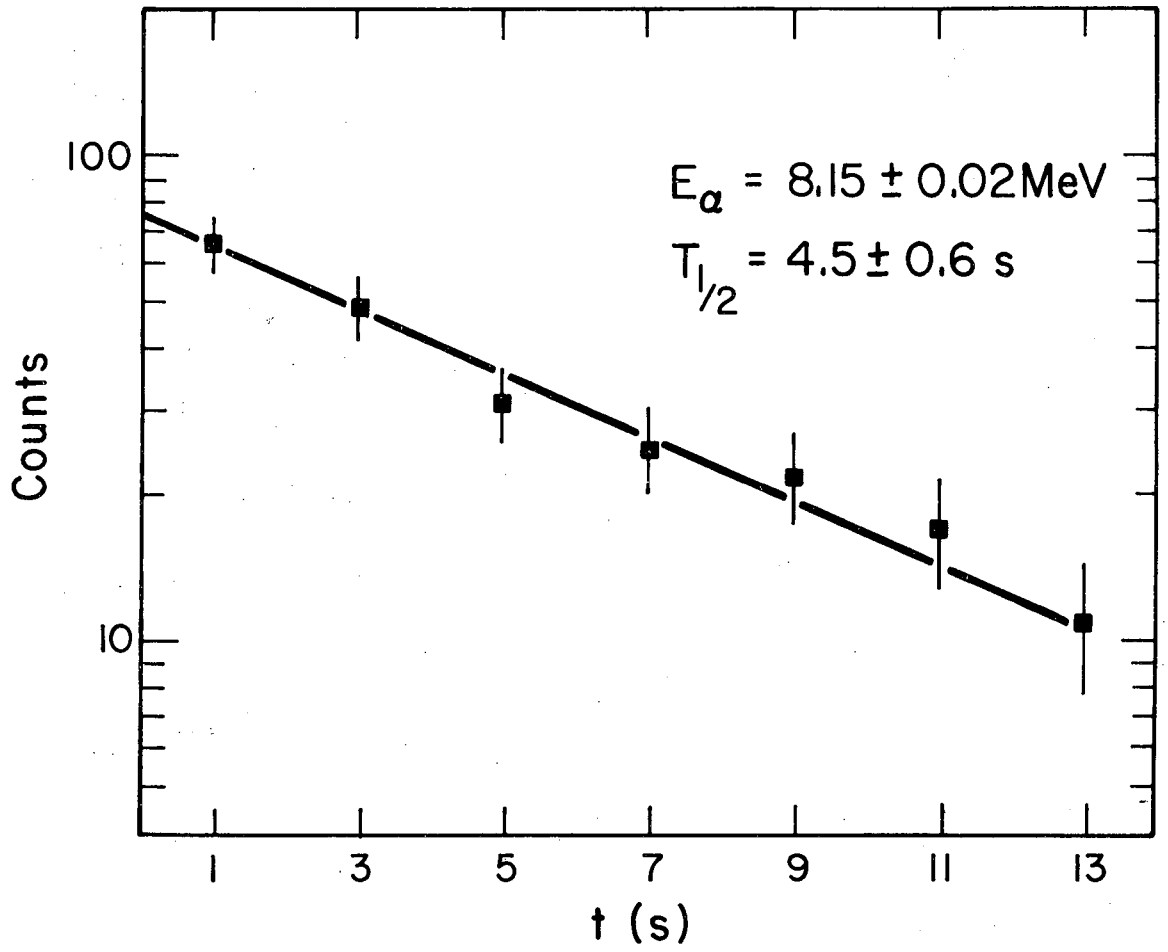

XBL 775-1027

Fig. 2

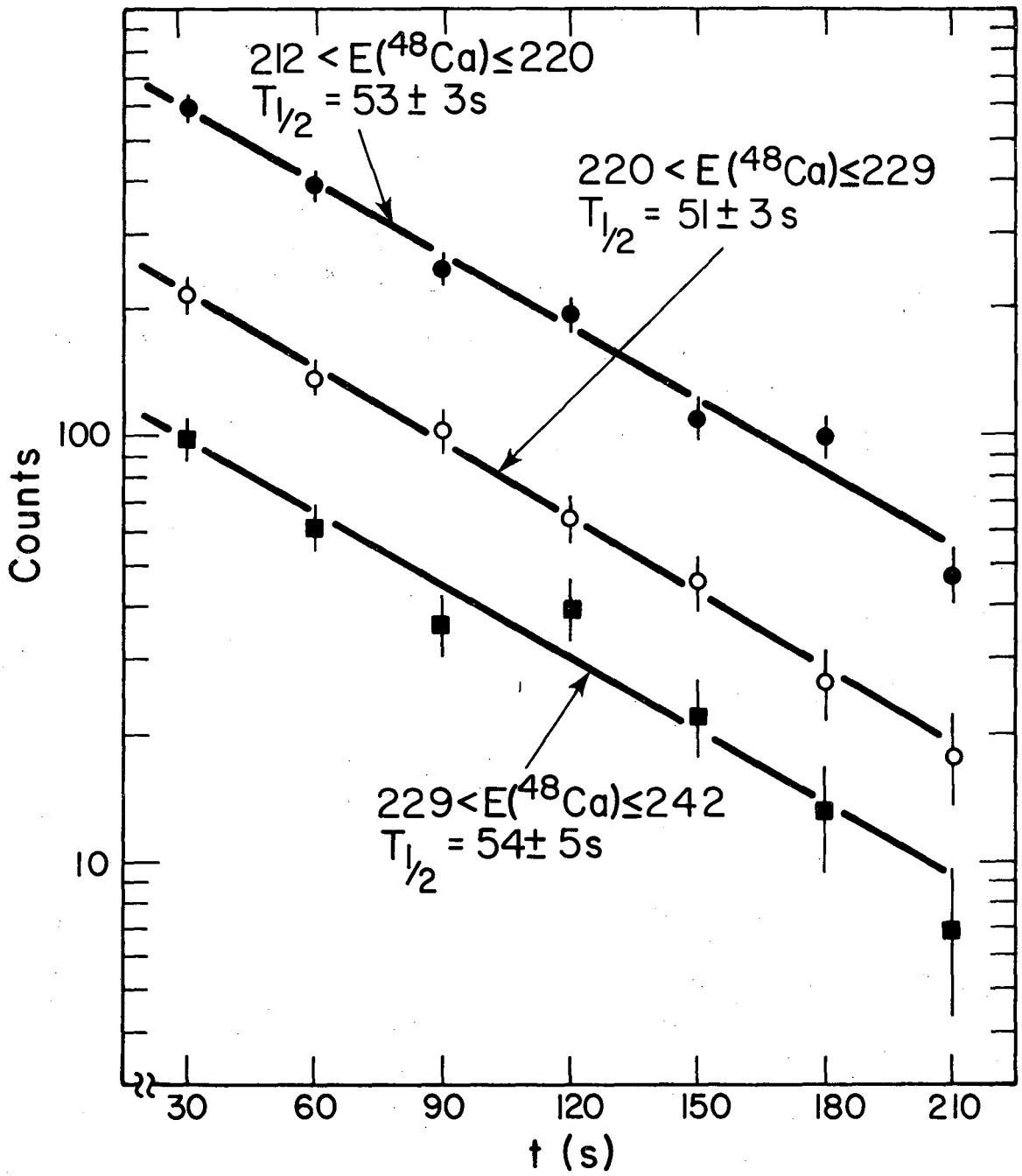

XBL 775-1028

Fig. 3

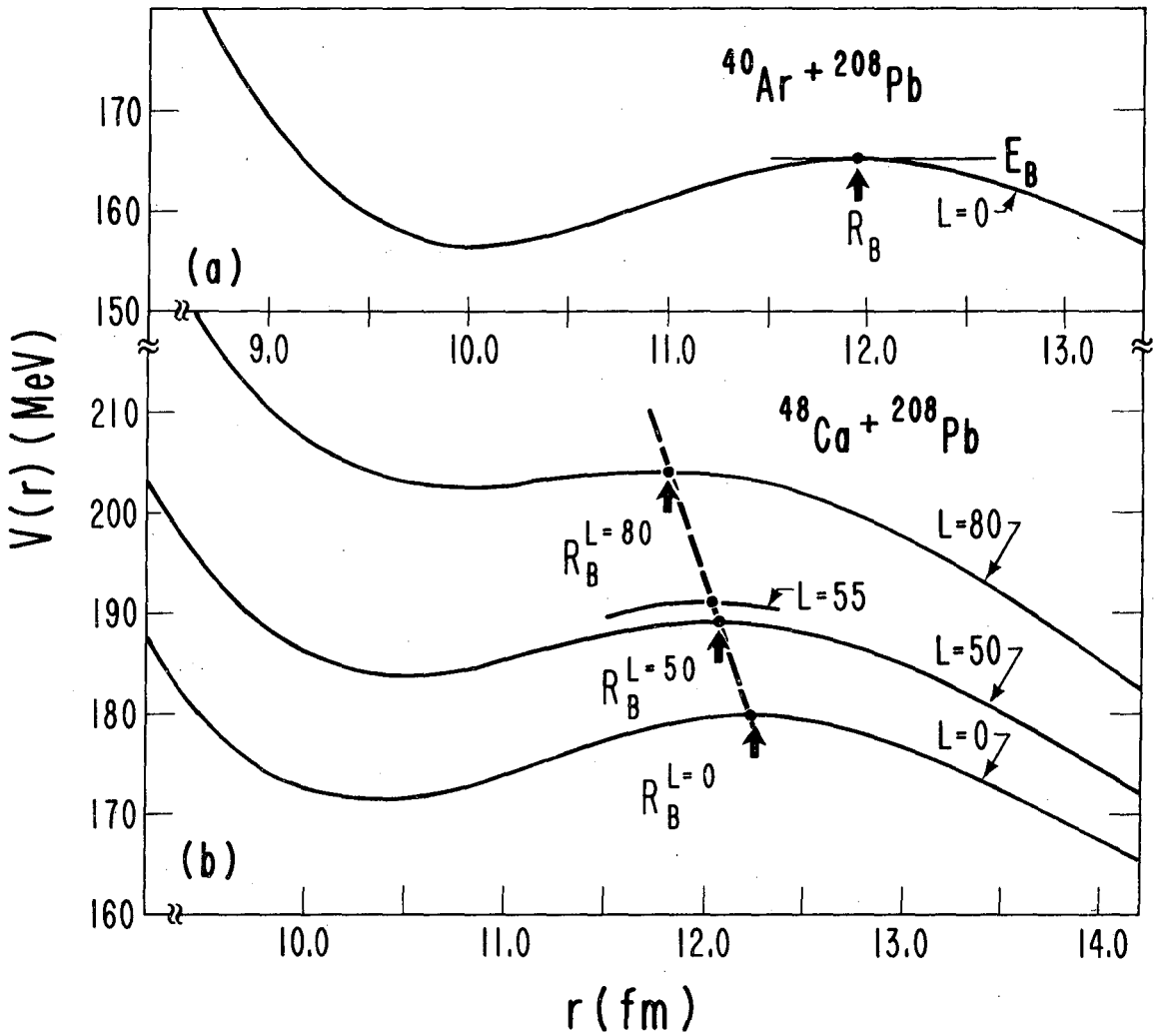

XBL 776-1084

Fig. 4

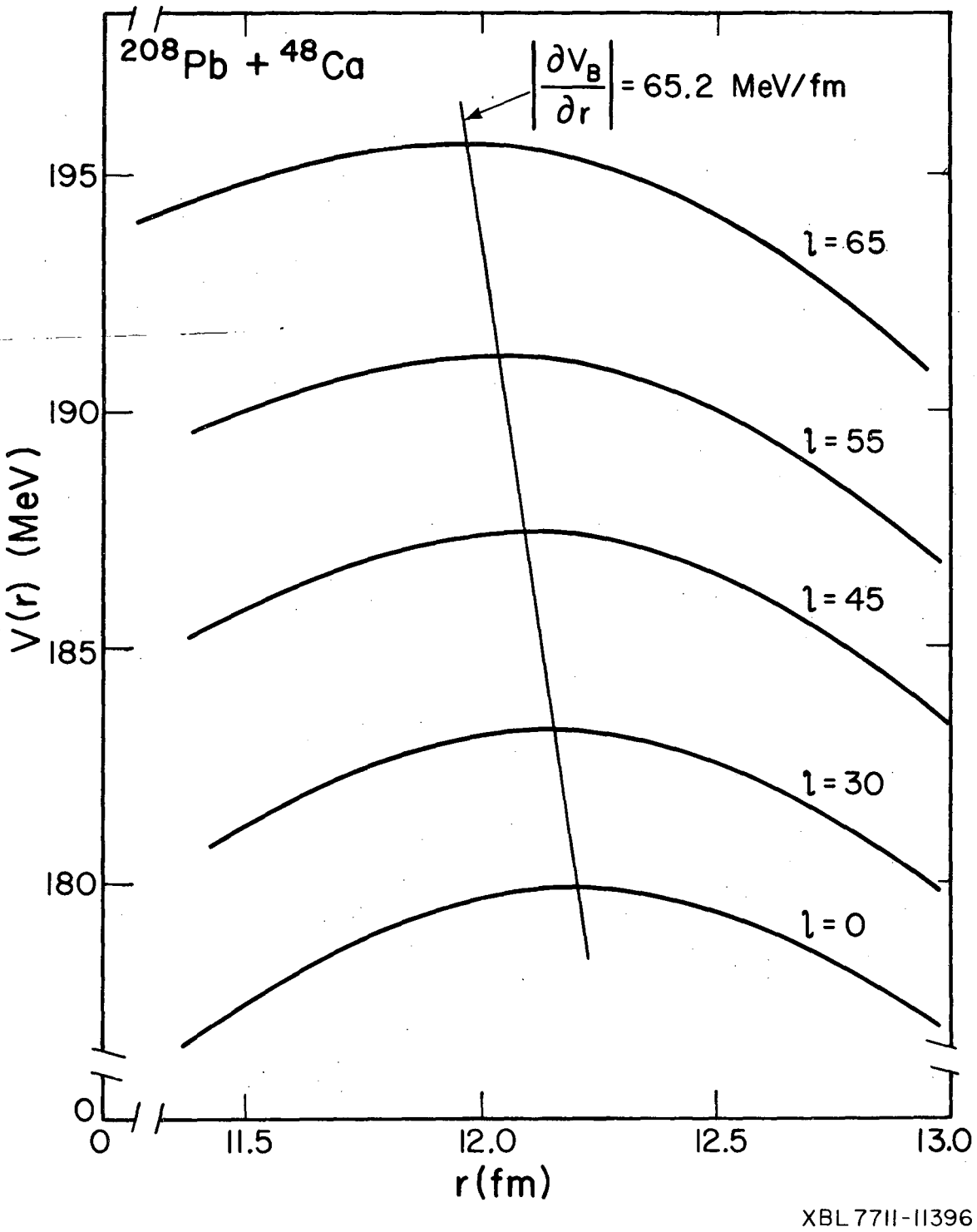
$^{208}Pb + ^{48}Ca$
$\left|\frac{\partial V_B}{\partial r}\right| = 65.2$ MeV/fm
195
190
185
180
0
V(r) (MeV)
l = 65
l = 55
l = 45
l = 30
l = 0
0
11.5
12.0
12.5
13.0
r (fm)
XBL 7711-11396

Fig. 5

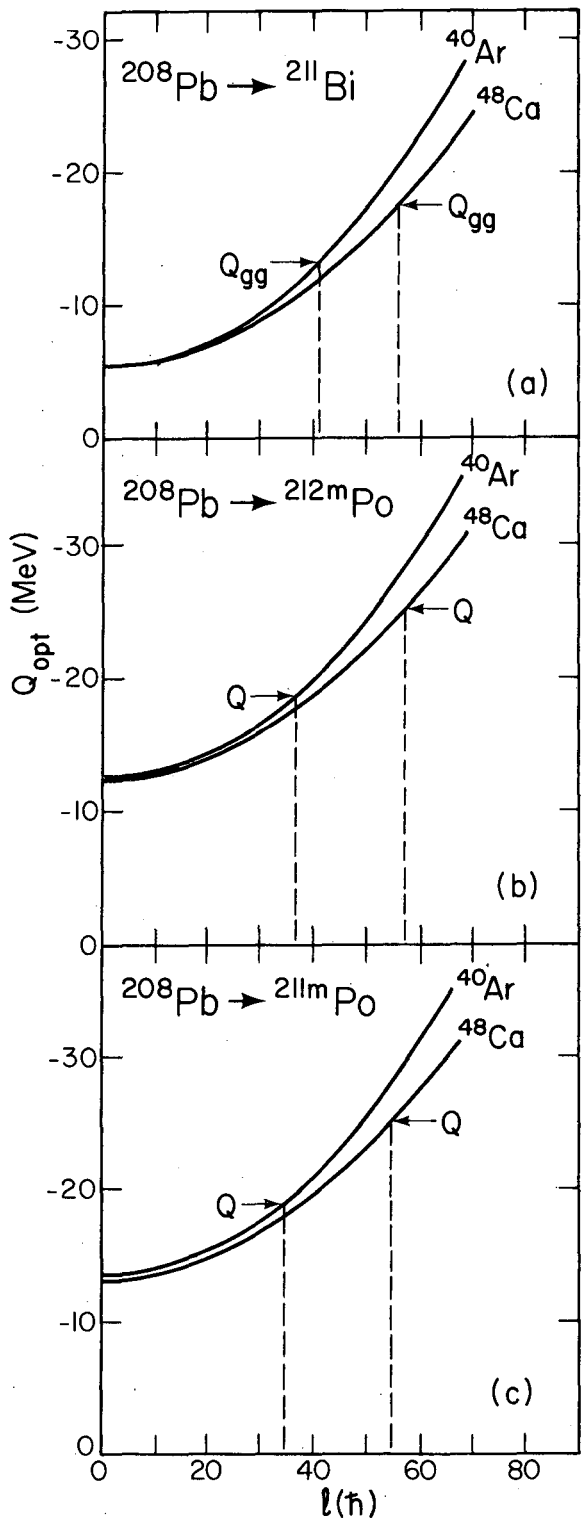

XBL 7711-11397

Fig. 6

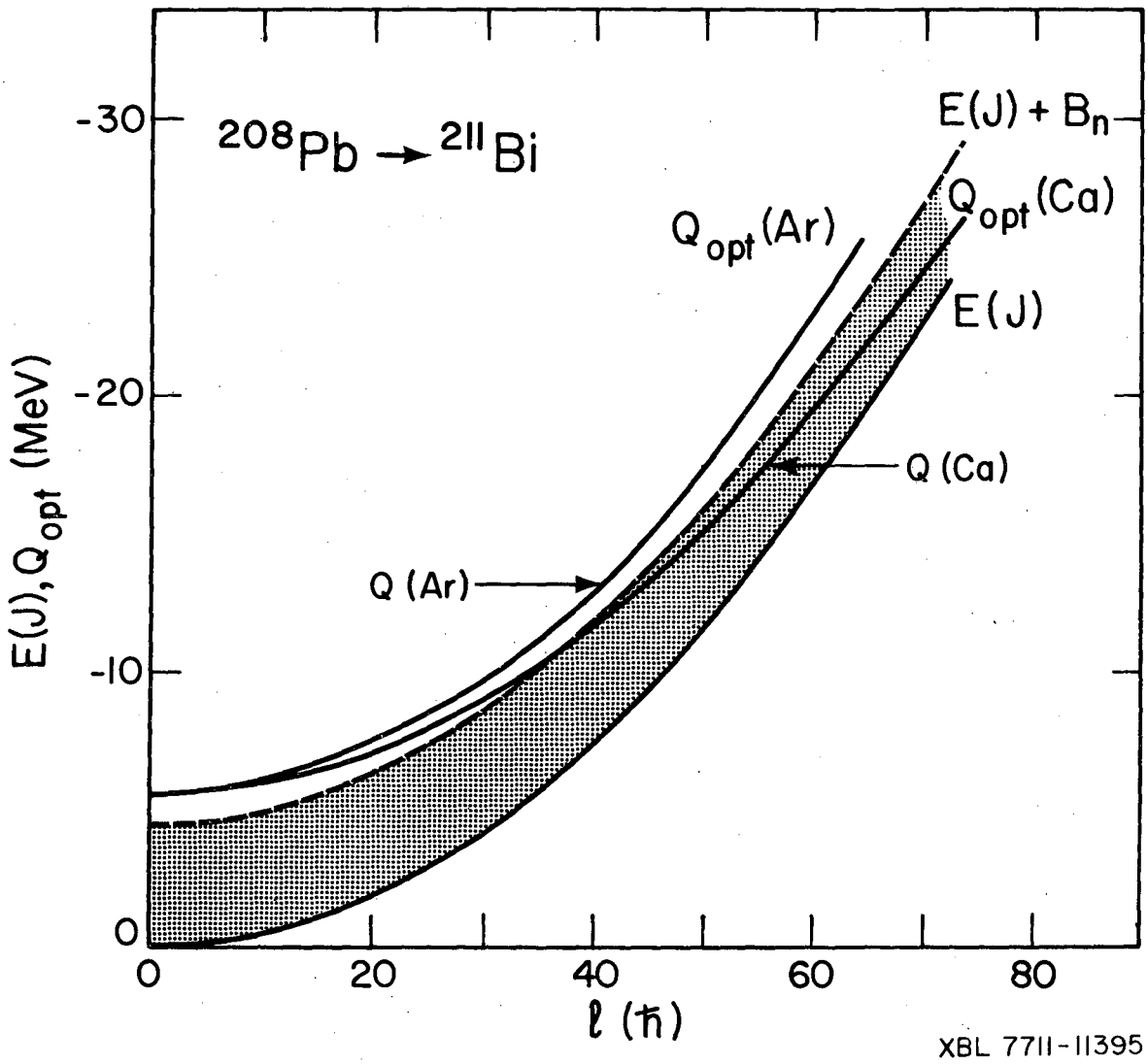
$^{208}Pb \rightarrow ^{211}Bi$
E(J) + B_n
Q_{opt}(Ar)
Q_{opt}(Ca)
E(J)
Q (Ca)
Q (Ar)
-30
-20
-10
0
0
20
40
60
80
E(J), Q_{opt} (MeV)
ℓ (ħ)
XBL 7711-11395

Fig. 7

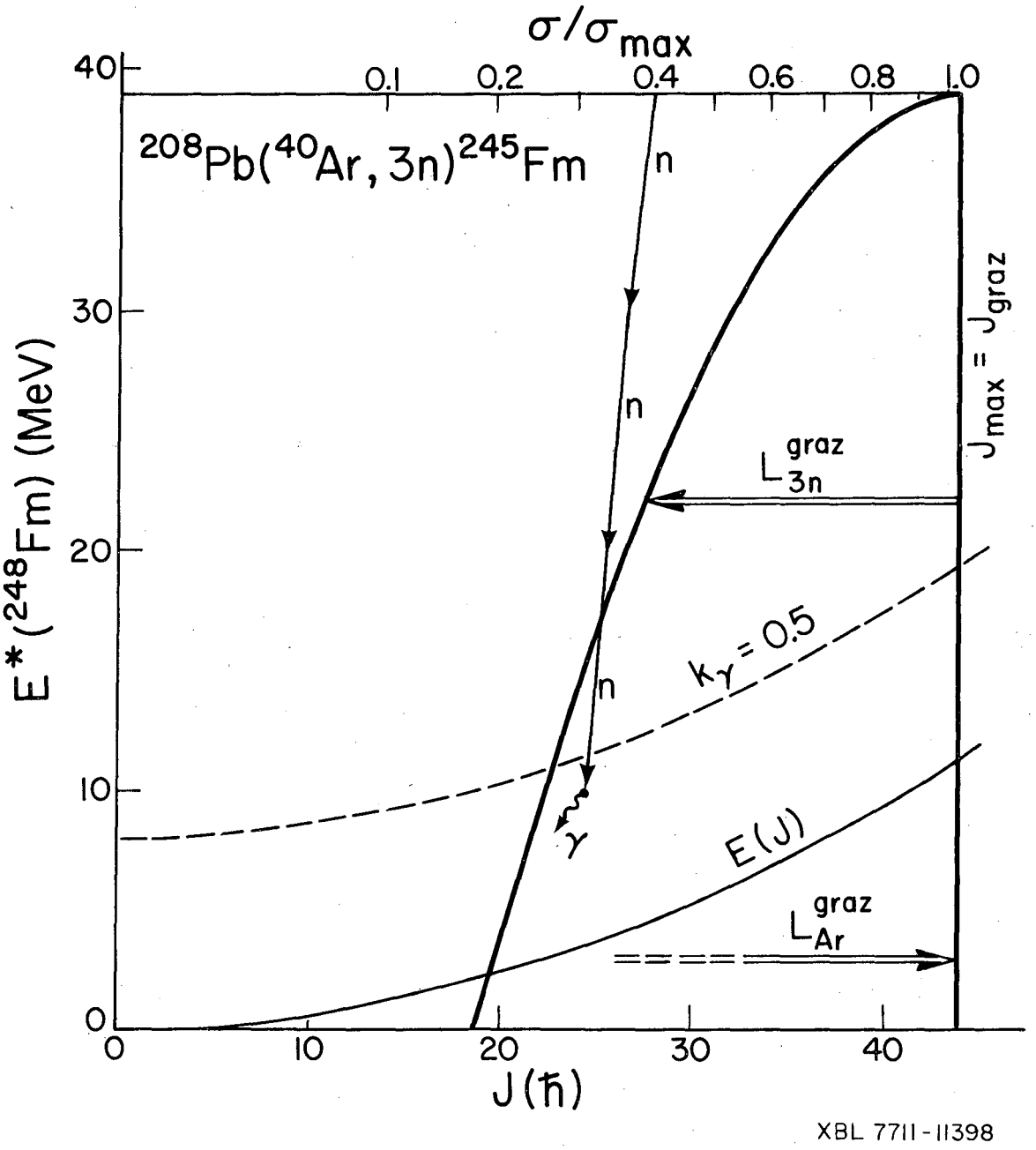
σ/σmax
0.1
0.2
0.4
0.6
0.8
1.0
208Pb(40Ar, 3n)245Fm
n
n
n
γ
Jmax = Jgraz
L3n graz
kγ = 0.5
E(J)
LAr graz
E*(248Fm) (MeV)
40
30
20
10
0
0
10
20
30
40
J(ħ)
XBL 7711-11398

Fig. 8

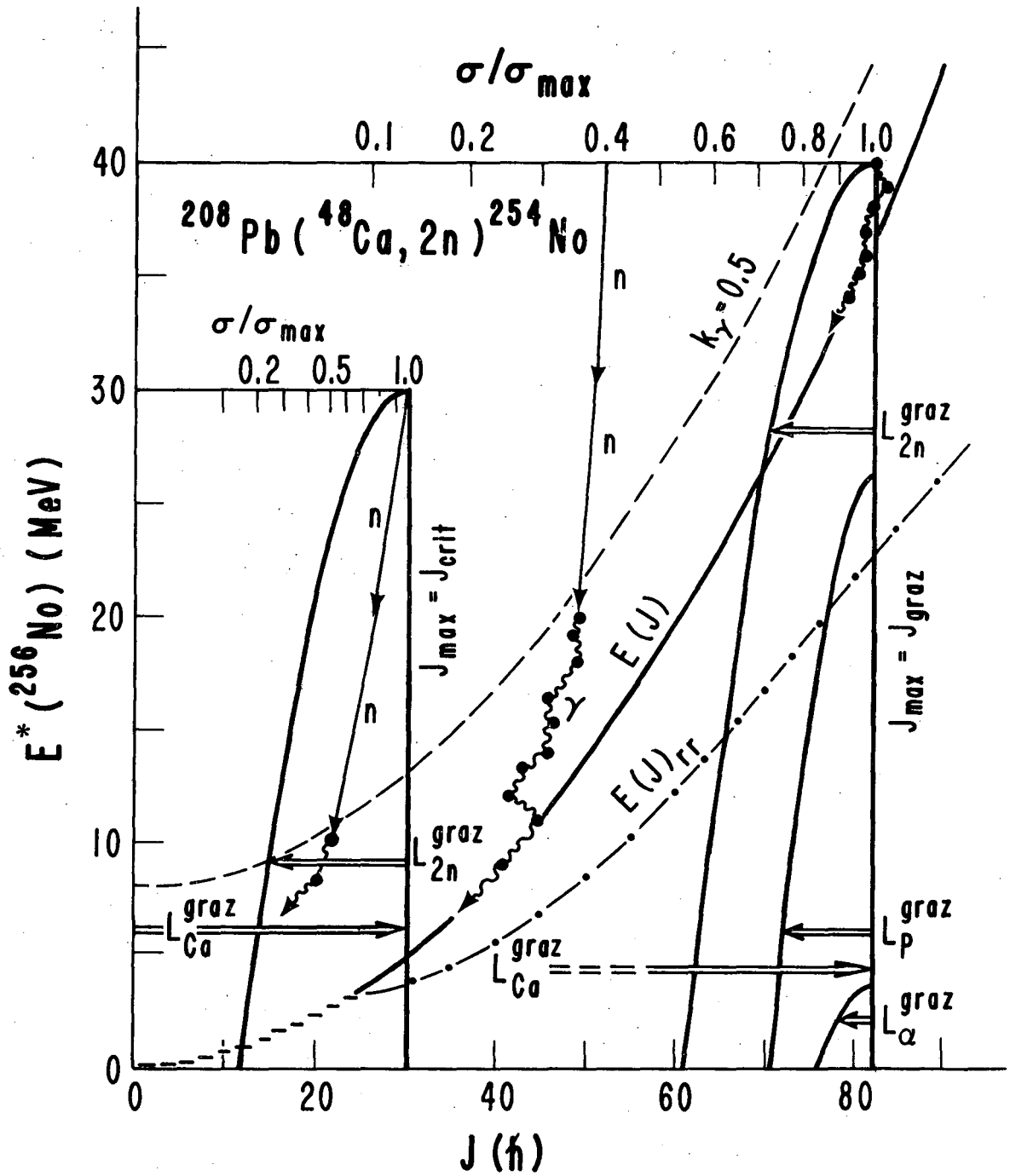

XBL 776-1083

Fig. 9

0 0 0 0 4 8 0 0 4 5 1

This report was done with support from the Department of Energy. Any conclusions or opinions expressed in this report represent solely those of the author(s) and not necessarily those of The Regents of the University of California, the Lawrence Berkeley Laboratory or the Department of Energy.

TECHNICAL INFORMATION DEPARTMENT
LAWRENCE BERKELEY LABORATORY
UNIVERSITY OF CALIFORNIA
BERKELEY, CALIFORNIA 94720